

# Signorini’s contact model for deformable objects in haptic simulations

Christian Duriez, Claude Andriot  
CEA LIST  
SCRI  
Fontenay-aux-Roses, France  
christian.duriez@cea.fr

Abderrahmane Kheddar  
AIST/ISI-CNRS  
Joint Japanese-French Robotics Laboratory (JRL)  
Tsukuba, Japan  
abderrahmane.kheddar@aist.go.jp

**Abstract**— In this paper we consider deformable objects in haptic simulations. The physical simulation that drives haptic perception requires a good dynamic behavior. The inputs of the deformable model come from the treatment of the collision. We propose to focus on the contact restitution between deformable objects to guarantee “*physical and perceptual realism*” of the haptic feedback. Signorini, in 1933, proposed a physical model of contact for deformable objects interacting with rigid static bodies [11]. This paper shows that the Signorini’s model extends to contacts between two deformable objects using Gauss-Seidel resolution of complementarity problems. An interactive resolution of the overall formulation is presented and experienced on deformable objects using the finite linear-elements method.

## I. INTRODUCTION

Physically based simulations are supposed to be somehow based on measured physics’ laws. When simulations are interactive, the *physical realism* usually turns out to be a compromise between real-time constraints and the fidelity of the simulation results. Haptic feedback revealed the need of simulations able to achieve hundreds hertz of frequency rates. To satisfy such rates, the simulation’s physical fidelity and precision are relaxed. Haptic feedback and physically based animation require contact determination, contact topology and other physical parameters. Contact topology is linked to the contact space characterization that is based on discrete geometry and other physical parameters. Geometric characterization of the contact is based on its discrete representation; hence it can be complex if object’s geometry and the contact configuration is complex. This is unfortunately the case in industry virtual prototyping since the objects geometry can not be simplified excessively. Physical simulation has three main issues: dynamic behavior, collision detection and response. Each issue can be more or less time consuming according to many parameters (application context, adopted methodology, etc.). This work focuses on contact response. Some of various existing methods are discussed in the following items:

- *Time integration*: is said to be *event driven* when the collision events trigger the integration scheme by seeking the first contact’s time. This technique is often used to prevent object’s inter-penetration (see [3], [7]), [10]. Other approaches use constant time step integration and are called *time-stepping methods*. The

motion dynamic formulation solves for the contacts appearing between steps ([1], [12]).

- *Contact modeling*: unilateral contacts and induced impacts and frictions phenomenon lead to a class of mechanical problems known as *non-smooth mechanics*. This is called so because of the velocities discontinuities and the unilateral contact space. Consequently, contact’ and friction’ laws are often regularized. When contact forces are relates to virtual-penetrations’ depth measures (PDM), that can be a volume [9] or a distance [6], collision response and dynamics are called penalty-based methods. On the contrary, constraints-based methods formulate the constraints (also the unilateral ones) explicitly in the dynamic equations. This makes them more suited to non-smooth mechanics’ simulations.
- *Collision inputs*: The contact response is obviously related to the collision detection technique. Collision time or configuration of first impact can be estimated [10] with continuous methods. Some algorithms use also geometrical distance (proximity algorithms) or a penetration depth (discrete collision detection) between objects. Other ones use penetration volume.

In this presented work, we are using strict formulation of the Signorini’s problem to deal with contact between deformable objects. The formulation is made to be independent from the collision detection technique in order to be as generic as possible. Normally, only two data are needed for the resolution of the proposed formulation:

- 1) the direction and,
- 2) the spots of the contacts.

Nevertheless, additional data that could be obtained from a continuous collision detection algorithm can be exploited<sup>1</sup>. For experiments, we use a proximity distance algorithm. The proposed motion/deformation integration method uses a *time-stepping* technique. Indeed, since deformable objects are made of a relatively high number of meshes, the contact configuration between deformable objects induces an important number of geometrical features (in our application, we experienced up to 50 instantaneous contacts within one spot). Moreover, the contact topology and configuration are very dynamic. Consequently it is difficult to find a mapping

<sup>1</sup>For instance, the geometric configuration at the impact time.

from the contact space to an equivalent reduced sub-space (as is the case with rigid bodies).

## II. SIGNORINI'S PROBLEM

Signorini described the contact between a deformable object in a rigid environment. This formulation is extended to solve contacts between deformable bodies.

### A. Theory

Let us consider the deformation of an elastic body in contact with a rigid surface<sup>2</sup>. The deformations are due to elementary volume forces  $\underline{df}_v$  (like its actual weight<sup>3</sup>  $\underline{df}_v = \varrho \cdot \underline{g}$ ), and to elementary surface forces  $\underline{df}_s$  that give, by integration, the contacts forces on contact points  $\underline{F}_C$ . The reference configuration of the object is  $\Omega \subset \mathbb{R}^3$  and the displacement of every point  $P$  from this configuration to the deformed configuration will be given by the function  $u(P) : \Omega \rightarrow \mathbb{R}^3$ . Inside the field  $\Omega$ , we have:

$$\text{div}(\underline{\sigma}) + \underline{df}_v = 0 \quad (1)$$

where  $\underline{\sigma}$  is the inside stress of the object. Here, we consider that the objects are perfectly elastic and isotropic. Thus, we can use the Hooke's law:

$$\underline{\sigma} = 2\mu\underline{\underline{\varepsilon}} + \lambda \text{tr}(\underline{\underline{\varepsilon}})I_d \quad (2)$$

with  $\underline{\underline{\varepsilon}}$  being the strain tensor,  $\mu$  and  $\lambda$  are the Lamé coefficient that are directly linked to the Young modulus  $E$  and to the Poisson coefficient  $\nu$  of the material.  $I_d$  is the  $3 \times 3$  identity matrix. The constraint is related to displacements thanks to a tensorial relation. We are using the well known Green-Lagrange tensor:

$$\varepsilon_{ij} = \frac{1}{2} \left( \frac{\delta u_i}{\delta x_j} + \frac{\delta u_j}{\delta x_i} \right) + \frac{1}{2} \left( \frac{\delta u_i}{\delta x_j} \times \frac{\delta u_j}{\delta x_i} \right) \quad (3)$$

with  $1 \leq i, j \leq 3$ . In the case of small displacements, the second part of the tensor can be neglected.

On the surface  $\delta\Omega$  of the object, the stress tensor<sup>4</sup> must be equilibrated with the contact forces to keep continuity at the limits. These contact forces are an integration of elementary surface forces  $\underline{df}_s$  that exert on the elementary surfaces  $ds$  along the normal  $\underline{n}$ , that is:

$$\underline{df}_s = -\underline{\sigma} \cdot \underline{n} \cdot ds = -\underline{\sigma}_s \cdot ds \quad (4)$$

Two types of surface stress are then distinguished, the normal stress, projected on the normal space:

$$\underline{\sigma}_s \cdot \underline{n} = \sigma_n \quad (5)$$

The normal stress is an unknown of the Signorini's problem. The shearing stress is the second type of surface stress:

$$\underline{\sigma}_s \cdot \underline{t} = \sigma_t \quad (6)$$

In this study, only frictionless contacts are considered, so the shearing stress is null. We suppose the existence

<sup>2</sup>For the notations, noted sizes  $\underline{\underline{T}}$  indicate the tensors and noted sizes  $\underline{v}$ , indicate the vectors

<sup>3</sup> $\varrho$  being the mass volume density and  $\underline{g}$  the gravity

<sup>4</sup> $\underline{\sigma}_s$  is homogeneous to a pressure

of an efficient contact topology algorithm<sup>5</sup>, which is able to delimit, characterize, and return part of object's surface ( $\delta\Omega$ ), named  $\xi$ , where the deformable object is *potentially* in contact. In fact more than simple collision detection is needed. We experienced that the resolution of the contact at one collision spot may create news contacts (at the neighborhood) or even new spots. This is why a proximity detection method is more suitable.

With the Signorini's formulation, the conditions of contact are obtained, for every point of the surface  $\xi$  ( $\forall P \in \xi$ ):

$$\begin{aligned} 0 \leq \delta_n(P) \perp \sigma_n(P) \geq 0 \\ \sigma_t(P) = 0 \end{aligned} \quad (7)$$

where  $\delta_n$  represents the minimal distance function between every point  $P$  of  $\xi$  and its near surrounding.

In the Signorini's formulation, for every point  $P$  of  $\xi$ , two states may be distinguished:

- either, the point  $P$  is actually a contact point, then  $\delta_n(P) = 0$  and  $\sigma_n(P) > 0$  or,
- the point  $P$  is not yet a contact point, then  $\delta_n(P) > 0$  and  $\sigma_n(P) = 0$ .

### B. Finite element method

Virtual objects deformation is computed using the well known finite element method. A brief recall of the method is proposed. The first step is to use a variational formulation of the continuum mechanics' equations. Let  $\Psi : \mathbb{R}^3 \rightarrow \mathbb{R}^m$  be the test function.

$$\text{div}(\sigma) + F_v = 0 \Leftrightarrow \iiint_{\Omega} \Psi (\text{div}(\sigma) + F_v) \partial\Omega = 0, \forall \Psi \quad (8)$$

The Green-Ostrogradski theorem allows rewriting the precedent equation separating the volume from the edge. That is:

$$\iiint_{\Omega} \Psi \cdot \text{div}(\sigma) \partial\Omega = \iiint_{\Omega} \sigma \cdot \text{grad}(\Psi) \partial\Omega + \iint_S \Psi \cdot \sigma_s \partial S \quad (9)$$

For now, we have only equivalences with the proviso of checking the condition " $\forall \Psi$ ". The Galerkin method proposes to verify the conditions only with some well chosen " $\Psi$ ". In this method, the chosen functions are those which are used for elements interpolation.

In the finite elements method, the position of a point inside an element depends on the position of the nodes and on the interpolation functions. In our case, we found some interest in using linear interpolation functions using tetrahedrons with four nodes. Although not very precise, when combined with the contact model, they allow the use of surface forces without an explicit integration on contact surface (which will be developed in the following section).

### C. Contact problem with linear elements

The Signorini's problem formulation in the context of the continuum mechanics enables to model the contact.

<sup>5</sup>May be part of the collision detection.

The FEM uses a variational formulation to integrate the equations from continuum formulation. We also use the finite element discretization to solve the Signorini's problem in a fast manner.

1) *2D example*: First, we prove that with linear elements in  $\mathbb{R}^2$ , the contact forces can be integrated easily along the objects surface (see the figure 1).

$$\int_l \Psi \sigma_n \cdot \partial x \quad (10)$$

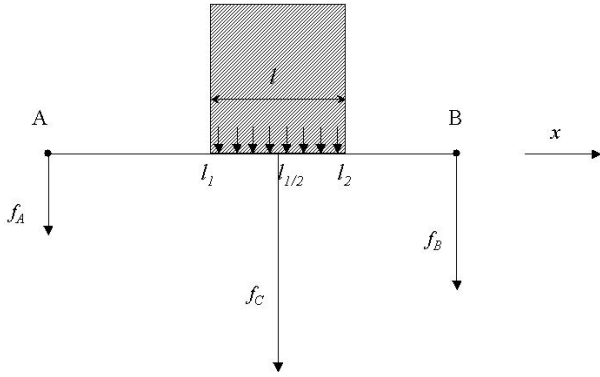


Fig. 1. Contact forces interpolation along the surface of a 2D linear element.

At the beginning of the contact forces computing process, we do not know both the external forces applied to the deformable object, and the final displacements of the nodes  $A$  and  $B$ . Hence,  $f_A$ ,  $f_B$ ,  $U_A$  and  $U_B$  are the unknowns of the system after discretization by the FEM (see the figure 1). However, we know that:

$$\begin{aligned} \int_l \Psi_A \sigma_n \partial x &= -f_A \\ \int_l \Psi_B \sigma_n \partial x &= -f_B \end{aligned} \quad (11)$$

Moreover, with linear elements,  $\sigma_n$  is constant inside the element. The previous equations may be rewritten as:

$$\begin{aligned} \int_l \Psi_A \sigma_n \partial x &= \sigma_n \int_l \Psi_A \partial x \\ \int_l \Psi_B \sigma_n \partial x &= \sigma_n \int_l \Psi_B \partial x \end{aligned} \quad (12)$$

It is known, using the Gauss points' integration method, that the value of the integral  $\int_x \Psi_A \partial x$  with the linear function  $\Psi$ , can be evaluated exactly with a single value in the middle of the interval:

$$\int_l \Psi_A \partial x = \int_{l_1}^{l_2} (a_0 + a_1 x) \partial x = (l_2 - l_1) \left( a_0 + a_1 \frac{l_2 + l_1}{2} \right) \quad (13)$$

Thus, with linear elements, the value of the surface forces is completely defined only with the force  $f_c$  exerted at the point  $l_{1/2}$

$$\begin{aligned} f_c &= -\sigma_n l \\ f_A &= -\sigma_n l \Psi_A(l_{1/2}) \\ f_B &= -\sigma_n l \Psi_B(l_{1/2}) \end{aligned} \quad (14)$$

But the forces are not the only unknowns of the Signorini's problem. The displacement must be also taken into account:

$$U_c = \Psi_A(l_{1/2})U_A + \Psi_B(l_{1/2})U_B \quad (15)$$

Thus, in this simple case, the Signorini's problem is discretized by the force and displacement unknowns in the middle of the element, using the same interpolation function than inside the element.

2) *3D generalization*: The simple 2D example is generalized here with two deformable objects  $O_1$  and  $O_2$ . We suppose that the CD algorithm (or the proximity detection) returns  $m$  contact' pairs. For every contact  $i \in [1, m]$ , a contact normal is also provided. Every contact connects a point  $P$  of the object  $O_1$  surface to a point  $Q$  of the object  $O_2$  surface.

Initially, it is assumed that these points are in the middle of contact surfaces like Gauss' points. We will see in the following section how to keep correct results if the CD algorithm falls to localize the "medium" of contact surfaces.

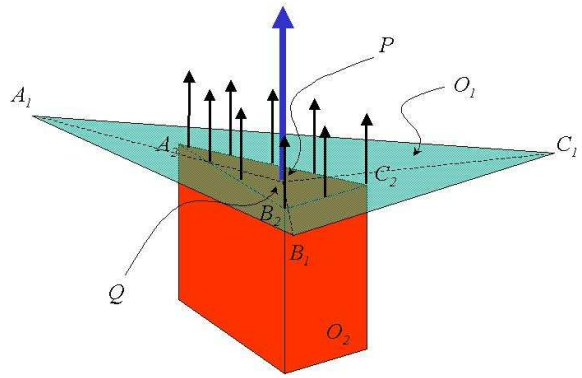


Fig. 2. Contact forces interpolation in 3D.

Each contact point provided by the CD is interpolated within the nodes of the element it belongs to. The points are necessarily on the surface of the objects, in other words, on a triangle. Let the triangle  $(A_1B_1C_1)$  (see the figure 2) be the support for the point  $P$ :

$$U_P = \Psi_{A_1}(P)U_{A_1} + \Psi_{B_1}(P)U_{B_1} + \Psi_{C_1}(P)U_{C_1} \quad (16)$$

In the same way, for  $(A_2B_2C_2)$  and  $Q$ :

$$U_Q = \Psi_{A_2}(Q)U_{A_2} + \Psi_{B_2}(Q)U_{B_2} + \Psi_{C_2}(Q)U_{C_2} \quad (17)$$

As the interpolation functions are linear inside the elements, one can use the barycenter of the contact's surface like a Gauss' point.

$$\begin{aligned} f_P &= -\sigma_n S \\ f_{A_1} &= f_P \Psi_{A_1}(P) \\ f_{B_1} &= f_P \Psi_{B_1}(P) \\ f_{C_1} &= f_P \Psi_{C_1}(P) \end{aligned} \quad (18)$$

And, similarly:

$$\begin{aligned} f_Q &= -f_P \\ f_{A_2} &= f_Q \Psi_{A_2}(Q) \\ f_{B_2} &= f_Q \Psi_{B_2}(Q) \\ f_{C_2} &= f_Q \Psi_{C_2}(Q) \end{aligned} \quad (19)$$

$S$  is the contact's surface. With two deformable objects, there is necessarily an arbitrary choice for the direction of the unknown force. We take the direction  $\underline{n}$  for which  $f_P$

is positive. It corresponds to the force that the object  $O_2$  exerts on  $O_1$ .

$$f_P = -f_Q = f_c \quad (20)$$

In the contact space, the force  $f_c$  is scalar. It will be projected on the contact normal. By processing the product of the scalar by the normal, the external force applied on the FEM appears as:

$$\begin{aligned} \frac{F_{A_1}}{F_{A_2}} &= f_{A_1} \underline{n}, \frac{F_{B_1}}{F_{B_2}} = f_{B_1} \underline{n}, \frac{F_{C_1}}{F_{C_2}} = f_{C_1} \underline{n} \\ & \quad (21) \end{aligned}$$

To linearize the problem, we freeze each contact's direction during the current time step. The Signorini's problem will be solved by considering both gap  $\delta$  and force  $f_c$  as scalars.

$$\delta = \underline{n} \cdot \underline{QP} \quad (22)$$

Displacements  $U_P$  and  $U_Q$  are considered between the free motion (collision and the contact forces are not taken into account) and the constrained motion (after resolution of the Signorini's problem and the integration of the contact forces), hence:

$$\begin{aligned} n &= [n_x \quad n_y \quad n_z] \\ \delta &= n^T (U_P - U_Q) + \delta_f \end{aligned} \quad (23)$$

$\delta_f$  is the free distance between objects when no contact force are integrated:

$$\begin{aligned} U_P &= [\Psi_{A_1}(P) \quad \Psi_{B_1}(P) \quad \Psi_{C_1}(P)] \begin{bmatrix} U_{A_1} \\ U_{B_1} \\ U_{C_1} \end{bmatrix} \\ U_Q &= [\Psi_{A_2}(Q) \quad \Psi_{B_2}(Q) \quad \Psi_{C_2}(Q)] \begin{bmatrix} U_{A_2} \\ U_{B_2} \\ U_{C_2} \end{bmatrix} \end{aligned}$$

By stacking all these relations for each contact, one can write mapping matrices  $H_P$  and  $H_Q$ , from the contact space to the motion space:

$$\delta = [H_P][U_1] - [H_Q][U_2] + \delta_f \quad (24)$$

$U_1$  and  $U_2$  are displacements of the nodes involved in the contact. In the same way, by stacking all the forces relations (equations 18, 19 and 21), we have:

$$[F_1] = [H_P]^T F_C \quad (25)$$

$$[F_2] = -[H_Q]^T F_C \quad (26)$$

$F_1$  and  $F_2$  are the external forces applied on mesh's nodes  $O_1$  and  $O_2$  respectively.

To use a LCP solver, we need to build a linear relations linking the contact forces to the positions in the contact space. Different FEM deformation models have been proposed in computer haptics. However to our best knowledge, it is always possible to find a constant matrix  $C_O$ , at the beginning of the time step, having linear relation between constrained positions of mesh's nodes  $P_c$  and the external

contact forces  $F$  on these nodes. Furthermore, positions obtained from free motion  $P_f$  appear in the expression.

$$P_c = C_O F + P_f$$

More details can be found in [5]. This system is condensed on the only nodes involved by the contact. Finally, the expected linear relation is written in the form:

$$\delta = ([H_P]C_{O_1}[H_P]^T + [H_Q]C_{O_2}[H_Q]^T) \times F_C + \delta_f \quad (27)$$

If more than two objects are in contact at the same time step, we have to use a formulation by contact groups. All the mapping matrices  $H_i$  of contact  $i$  are stacked into a global matrix  $H$ , and each object  $j$  compliance matrix  $C_j$  are stacked into a global matrix  $C$ . Then, for every contact group, this formulation leads to the following LCP:

$$\begin{cases} F_C \geq 0 \\ \delta = (HCH^T)F_C + \delta_f \geq 0 \\ F_C \perp \delta \end{cases} \quad (28)$$

### III. RESOLUTION AND DISCUSSION

#### A. Gauss-Seidel local resolution

With linear elements, only one point of contact allows integrating the pressure force on the surface. However, we notice that it is advantageous to solve with the maximum number of contact points. Indeed, by taking again our 2D example and the equation 14:

$$\int_l \Psi_A \partial x = l \frac{\Psi_A(l_1) + \Psi_A(l_2)}{2} = l \Psi_A \frac{l_1 + l_2}{2}$$

If the contact is solved using  $l_1$  and  $l_2$  as points of Gauss for integrating the contact pressure, the solution of the Signorini's problem will be given by:

$$\frac{f_{C_1} + f_{C_2}}{2} = f_C$$

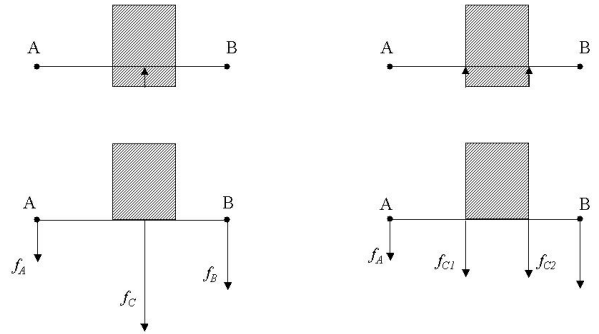


Fig. 3. 1D contact with one or two points for surface force evaluation.

If more than two points are used, the solution is not unique. Indeed several forces' solutions integrate the contact pressure correctly. In this case, the matrix  $HCH^T$ 's rank is not equal to  $m$ . Some LCP solvers use the matrix' full rank property to accelerate the process [8].

In order to be able to distribute the maximum of collision tests between the elements, we use an algorithm close to the Gauss-Seidel method for contacts resolution. This algorithm is very easy to implement and robust to converge

toward a solution even if several solutions are possible. The convergence is proved in [2]. The algorithm principle is to visit every contact, considering that the state of all the others is “frozen”. We can observe in equation 29 that if we “freeze” contact contribution for  $j \neq i$  this equation expresses a linear relation between  $\delta_i$  and  $f_i$ .

$$\delta_i = \delta_i^{free} + (HCH^T)_{ii}f_i + \sum_{j \neq i} (HCH^T)_{ij}f_j \quad (29)$$

If the present contact respects the Signorini’s problem, the force  $f_i$  is imposed to be zero, otherwise the force imposes a  $\delta_i$  equal to zero.

```

Input:  $\delta_{free}$ , HCH
Output:  $\delta$ , force
repeat
  foreach contact  $i$  in the list do
    displacement[ $i$ ] = 0
    foreach contact  $j$  except  $i$  do
      displacement[ $i$ ] += HCH[ $i$ ,  $j$ ] × force[ $j$ ]
     $\delta[i] = \delta_{free}[i] + displacement[i]$ 
    if ( $\delta[i] > 0$ ) then
      force[ $i$ ] = 0
    else
      force[ $i$ ] =  $-\delta[i]/HCH[i, i]$ 
until fixed number of iterations reached;

```

The algorithm processing must keep the same ordering in the contacts’ list. Nevertheless, if the same contact is put twice in the list, the algorithm will eventually put a force on the first. But the second will always respect the Signorini’s problem with no added force. From experimental data<sup>6</sup>, it appears that with seventy contacts and a hundred loops, convergence is reached in less than 1ms. Whereas the time spent to build the LCP is longer (about 5ms).

### B. Multi-resolution of contact and deformation meshes

The presented model uses linear element interpolation functions to map the contact space to the motion one. We showed that contact points can be considered as Gauss’ points to easily integrate, on mesh nodes, contact pressures into external forces. We proposed an algorithm of LCP resolution that manages a “super-abundance” of contact points on the same element. However, our resolution is dependent on the contacts’ normal provided by the CD algorithm. In our application context, coarse meshes for FEM deformable models are often used to reach real-time constraints. This leads to non-regular contact surface between objects, and perturbs the haptic feedback. We manage a collision detection specific surface mesh that has more triangles than the FEM mesh.

Then, the interpolation of each *collision mesh*’ vertex is computed off-line within its corresponding *FEM mesh*’s element. This computation process saves considerable time in building the LCP. The building of the mapping matrices  $H$  (from the contact to the deformation spaces) should also take into account successive interpolations, that is:

<sup>6</sup>On a PIV at 2.6GHz with 500RAM.

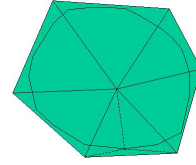


Fig. 4. Surface collision mesh interpolated in a FEM mesh.

- contact interpolation on a contact triangle;
- interpolation of each triangle’s vertex on the tetra element to which it belongs.

We noticed that this technique provides a solution for smoothing the meshes. To make honest physics deformations it is necessary to keep a significant number of degrees of freedom (dof) on the FEM mesh. As we adopted linear elements, the stress is constant along the surface. The topology of the contact will not be taken into account if there is a lack of dof (see the figure 5).

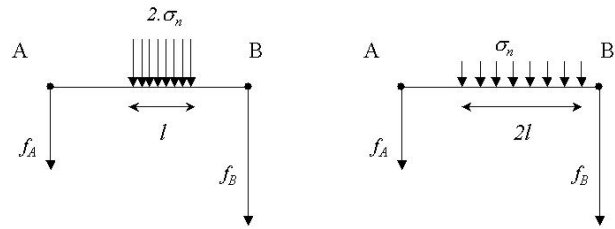


Fig. 5. Equivalent contact force pressure with linear element.

However, this may become a drawback if the considered elements are somehow large.

### C. Unfolding of a time step

In this section, the different stages of the computation are described. If non linear finite elements are used with an implicit integration, it is necessary to find the tangent to the deformation at the beginning of every time step. In practice, it is difficult to do this process in real time except for a reduce number of nodes. With an explicit integration, this is not necessary because the stress is calculated at the previous time step (see [5] for a more detailed discussion).

```

foreach time step  $t$  do
  if non-linear deformation then
    compute  $K(U_{t-1})$ 
    Free-Motion()
    Collision-Detection()
    LCP-Construction()
    Gauss-Seidel()
    Constrained-Motion()

```

If a haptic device is connected to a virtual deformable object, the free motion will integrate the applied forces by the user through the device. Other forces (like gravity) are also integrated. The collision detection gives contact normals and geometric configurations. Then, mapping matrices  $H$

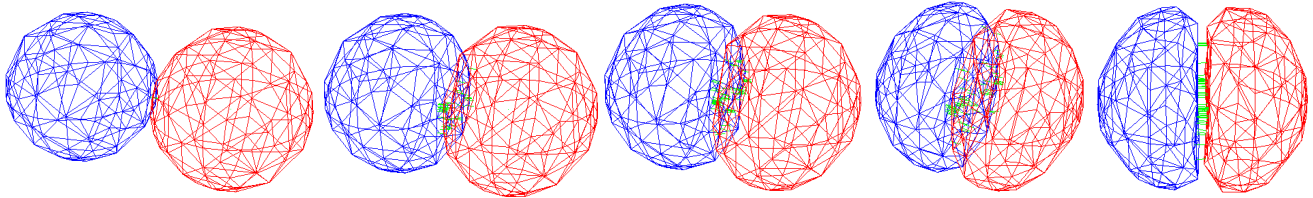


Fig. 6. Screen snapshots of two colliding spheres of similar stiffness.

are computed and  $HCH^T$  for every contact group; this is the most time consuming process after the collision detection one. Finally, the Gauss-Seidel algorithm solves for the Signorini's problem, and the contact forces are integrated to find constrained motion.

#### IV. RESULTS

The proposed method has been implemented using C++. The Virtuoso<sup>7</sup> device has been used to interactively manipulate objects and display interaction forces (figure 7).

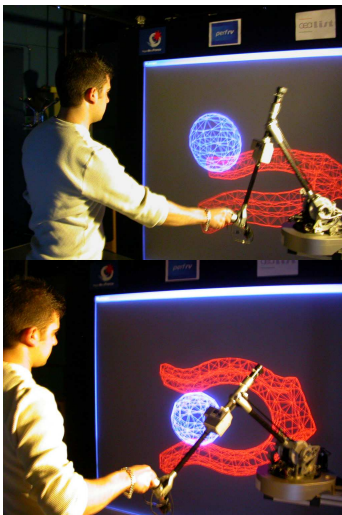


Fig. 7. Snap-in operation with haptic feedback

The figure 6 shows screen snapshots of interactive simulation of a pair of deformable spheres. One sphere is statically positioned and the other one is interactively manipulated by the operator; its trajectory is given by the haptic device. When the virtual spheres come into contact, interaction forces are computed and displayed to the operator. The simulation exhibits a truthful behavior as exhibited by the separating plane shape at the contact spot.

The figure 8 shows interaction of a deformable sphere with a deformable cylinder of lower stiffness. The contact area progressively shapes the sphere as being deformed. Real-time computation allows stable and transparent force feedback leading the operator to experience truly interactive manipulation of interacting deformable objects.

#### V. CONCLUSION

This paper presents an interactive deformable contact model for virtual reality applications with haptic feedback.

<sup>7</sup><http://www.haption.com/>

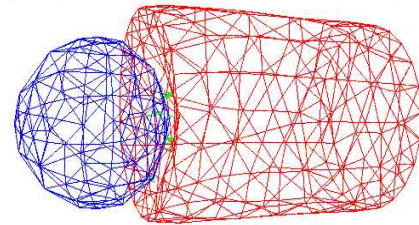


Fig. 8. A deformable ball interacting with a deformable cylinder.

The algorithm is an extension of the Signorini's theory on rigid/deformable contacts. The formulation of the deformation is based on linear FEM. Interactive manipulations with force feedback have been experienced.

Future work deals in including static and dynamic friction with more complex objects given from actual industry virtual prototyping scenarios. At this writing time we succeeded. We are investigating using nonlinear elements.

#### VI. ACKNOWLEDGMENTS

Authors thank to Frédéric Dubois from LMGC, Montpellier. This work is supported by the Région Ile-de-France.

#### REFERENCES

- [1] M. Anitescu, F.A. Potra, D.E. Stewart, *Time-stepping for three-dimensional rigid body dynamics*, Computational Methods in Applied Mechanical Engineering, vol. 177, no. 3-4, pp. 183-197, 1999.
- [2] P. Alart, A. Curnier, A mixed formulation for frictional contact problems prone to newton like solution methods. Computer Methods in Applied Mechanics and Engineering, vol. 7, 1992.
- [3] D. Baraff, *Fast contact force computation for non-penetrating rigid bodies*, ACM SIGGRAPH, Orlando, 1994.
- [4] R. Bridson, R. Fedkiw, and J. Anderson, *Robust Treatment of Collision, Contact and Friction for Cloth Animation* CM SIGGRAPH 2002.
- [5] C. Duriez, C. Andriot, and A. Kheddar, *A multi-threaded approach for deformable/rigid contacts with haptic feedback*, IEEE Haptic Symposium, 2004.
- [6] S. Fisher, M.C. Lin, *Fast Penetration Depth Estimation for Elastic Bodies Using Deformed Distance Fields*, IEE/RSJ IROS, March, 2001.
- [7] B. Mirtich, J. Canny, *Impulse-based Simulation of Rigid Bodies*, In Proceedings of Symposium on Interactive 3D Graphics, April 1995.
- [8] K.G. Murty, *Linear Complementarity Programming*, Internet Edition, 1998.
- [9] J.F. O'Brien, *Graphical Modeling and Animation of Fracture*, PhD Thesis, Georgia Institute of technology, July 2000.
- [10] S. Redon, A. Kheddar, S. Coquillart, *Gauss least constraints principle and rigid body simulations*, IEEE International Conference on Robotics and Automation, May 11-15, Washington DC, USA, 2002.
- [11] S. Signorini, *Sopra alcune questioni di elastostatica* Atti della Societa Italiana per il Progresso delle Scienze, 1933.
- [12] D.E. Stewart, J.C. Trinkle, *An Implicit Time-Stepping Scheme for Rigid Body Dynamics with Inelastic collisions and Coulomb Friction*, International Journal of Numerical Methods in Engineering, vol. 39, pp. 2673-2691, 1996.